npj | Quantum Information

www.nature.com/npjqi

ARTICLE OPEN

Check for updates

Sudden death and revival of Gaussian Einstein–Podolsky–Rosen steering in noisy channels

Xiaowei Deng[1,2,4], Yang Liu[1,2,4], Meihong Wang[2,3], Xiaolong Su[2,3]✉ and Kunchi Peng[2,3]

Einstein–Podolsky–Rosen (EPR) steering is a useful resource for secure quantum information tasks. It is crucial to investigate the effect of inevitable loss and noise in quantum channels on EPR steering. We analyze and experimentally demonstrate the influence of purity of quantum states and excess noise on Gaussian EPR steering by distributing a two-mode squeezed state through lossy and noisy channels, respectively. We show that the impurity of state never leads to sudden death of Gaussian EPR steering, but the noise in quantum channel can. Then we revive the disappeared Gaussian EPR steering by establishing a correlated noisy channel. Different from entanglement, the sudden death and revival of Gaussian EPR steering are directional. Our result confirms that EPR steering criteria proposed by Reid and I. Kogias et al. are equivalent in our case. The presented results pave way for asymmetric quantum information processing exploiting Gaussian EPR steering in noisy environment.

npj Quantum Information (2021)7:65 ; https://doi.org/10.1038/s41534-021-00399-x

INTRODUCTION

Nonlocality, which challenges our comprehension and intuition about the nature, is a key and distinctive feature of quantum world. Three different types of nonlocal correlations: Bell nonlocality[1], Einstein–Podolsky–Rosen (EPR) steering[2–6], and entanglement[7] have opened an epoch of unrelenting exploration of quantum correlations since they were introduced. The notion of EPR steering was introduced as the phenomenon that one can remotely steer the (conditional) quantum state owned by the other party through local measurements on half of an entangled state[2,3]. According to the hierarchy of nonlocality, EPR steering stands between entanglement and Bell nonlocality[8]. The existence of steering does not imply the violation of any Bell inequality, while the violation of at least one Bell inequality immediately implies steering in both directions, which is referred as two-way steering[9]. Remarkably, there is a situation that a quantum state may be steerable from Alice to Bob, but not vice versa, which is called the one-way steering[9–17]. This intriguing feature comes from the intrinsically asymmetric with respect to the two subsystems.

The one-way EPR steering has been observed for both continuous variable (CV)[9–13] and discrete variable (DV) systems[14–17]. Gaussian states and Gaussian operations play a central role in the analysis and implementation of CV quantum technology[18,19]. When considering generally bipartite Gaussian states and using Gaussian measurements, the steerability between the submodes is referred as Gaussian steering. What is more interesting, it has been shown that the direction of Gaussian EPR steering can be manipulated in noisy environment[12]. The temporal quantum steering and spatio-temporal steering have also been investigated[20–22]. Very recently, the EPR steering using hybrid CV and DV entangled state[23] and remote generation of Wigner-negativity through EPR steering[24] are demonstrated. As applications, EPR steering has been identified as an essential resource for one-sided device-independent quantum key distribution[25–27], quantum secret sharing[28,29], secure quantum teleportation[30–32], securing quantum networking tasks[33], and subchannel discrimination[34,35].

Besides two-mode EPR steering, the multipartite EPR steering has also been widely investigated since it has potential application in quantum network. Genuine multipartite steering exists if it can be shown that a steering nonlocality is necessarily shared among all observers[36]. The criterion for multipartite EPR steering and for genuine multipartite EPR steering has been developed[36,37]. Genuine high-order EPR steering has also been experimentally demonstrated[38]. Multipartite Gaussian EPR steering in Greenberger–Horne–Zeilinger state[10,39] and a four-mode cluster state[11] have been demonstrated. The experiments of multipartite Gaussian EPR steering only demonstrated EPR steering in the case of bipartite splitting at present, while genuine multipartite EPR steering for Gaussian states has not been demonstrated. Recently, the distribution of multipartite steering in a quantum network by separable states has been demonstrated[40,41].

The performance of modern quantum communication sort of relies on the interaction between quantum system and environment, which is generally described by the theory of decoherence. Decoherence, caused by the loss and noise encountered in quantum channel, can destroy fragile quantum properties of quantum states, and thus the information carried by the quantum states will be affected. Decoherence effects on entangled state has been well studied[42–47]. It has been shown that two entangled qubits become completely separable in a finite-time under the influence of vacuum which is the so called entanglement sudden death[42,43], and disentanglement occurs in Gaussian multipartite entangled states when one mode is transmitted in a noisy channel[48]. It is essential to recover entanglement when entanglement sudden death happens. A number of methods to recover the destroyed entanglement have been demonstrated, such as the non-Markovian environment[48–50], weak measurement[51], and feedback[52]. Since EPR steering is so intriguing and has enormous potential in quantum communication applications, it is imperative and significant to investigate the influence on Gaussian EPR

[1]Shenzhen Institute for Quantum Science and Engineering, Southern University of Science and Technology, Shenzhen, China. [2]State Key Laboratory of Quantum Optics and Quantum Optics Devices, Institute of Opto-Electronics, Shanxi University, Taiyuan, China. [3]Collaborative Innovation Center of Extreme Optics, Shanxi University, Taiyuan, China. [4]These authors contributed equally: Xiaowei Deng, Yang Liu. ✉email: suxl@sxu.edu.cn

steering made by decoherence. In 2015, the decoherence of steering was theoretically investigated[53]. Furthermore, it is unknown whether the methods used to recover entanglement can be used to recover EPR steering when sudden death of EPR steering happens.

Here, we experimentally investigate the properties of Gaussian EPR steering for a two-mode squeezed state (TMSS) when it is transmitted in lossy and noisy quantum communication channels, respectively. First, we investigate the influence of purity of quantum states on Gaussian EPR steering. We show that in a lossy channel, the impurity of the state leads to decrease of steerabilities and two-way steering region, but it never leads to sudden death of Gaussian EPR steering. Second, we find the Gaussian EPR steering totally disappear at certain noise level in a noisy quantum channel, which demonstrates sudden death of EPR steering. Third, we successfully revive the Gaussian EPR steering after its sudden death by establishing a correlated noisy channel. We also confirm that the steering quantifier proposed by I. Kogias et al. and the steering criterion proposed by M. Reid are equivalent for a TMSS with Gaussian measurement. The presented results provide useful references for applying Gaussian EPR steering in noisy environment.

RESULTS

The principle

The state we use in the experiment is a deterministically prepared TMSS, whose quantum correlations between quadratures are expressed by $\Delta^2(\hat{x}_A+\hat{x}_B)=\Delta^2(\hat{p}_A-\hat{p}_B)=2e^{-2r}$, where $\hat{x}=\hat{a}+\hat{a}^\dagger$ and $\hat{p}=\left(\hat{a}-\hat{a}^\dagger\right)/i$ are the amplitude and phase quadratures of an optical mode, respectively, r is the squeezing parameter ranging from 0 to infinite which correspond to no squeezing and the ideal squeezing, respectively. Under this definition, the noise of the vacuum state is normalized to 1. All Gaussian properties of a TMSS can be described by its covariance matrix:

$$\sigma_{AB}=\begin{pmatrix} a & 0 & \gamma & 0\\ 0 & a & 0 & -\gamma\\ \gamma & 0 & \beta & 0\\ 0 & -\gamma & 0 & \beta \end{pmatrix}=\begin{pmatrix} \mathbf{A} & \mathbf{C}\\ \mathbf{C}^T & \mathbf{B}\end{pmatrix} \tag{1}$$

with $\sigma_{ij}=\mathrm{Cov}\left(\hat{R}_i,\hat{R}_j\right)=\frac{1}{2}\left\langle\hat{R}_i\hat{R}_j+\hat{R}_j\hat{R}_i\right\rangle-\left\langle\hat{R}_i\right\rangle\left\langle\hat{R}_j\right\rangle$, $i, j=1$–4, where $\hat{R}=\left(\hat{x}_A,\hat{p}_A,\hat{x}_B,\hat{p}_B\right)^T$ is a vector composed by the amplitude and phase quadratures of bipartite optical beams[18]. For the theoretical covariance matrix elements of the TMSS we used in the experiment, $\mathbf{A}=a\mathbf{I}$, $\mathbf{B}=\beta\mathbf{I}$, $\mathbf{C}=\gamma\mathbf{Z}$, $\mathbf{I}$ and $\mathbf{Z}$ are the Pauli matrices:

$$\mathbf{I}=\begin{pmatrix}1&0\\0&1\end{pmatrix},\mathbf{Z}=\begin{pmatrix}1&0\\0&-1\end{pmatrix} \tag{2}$$

and

$$\begin{aligned} a &= \tfrac{V_s+V_{as}}{2}\\ \beta &= \tfrac{V_s+V_{as}}{2}\\ \gamma &= \tfrac{V_s-V_{as}}{2}\end{aligned} \tag{3}$$

in which $V_s=e^{-2r}$ and $V_{as}=e^{2r}+\delta$ are the squeezing and anti-squeezing fluctuation of the initial squeezing state, respectively. The existence of δ is caused by classical and uncorrelated noise in quantum resource and leads to the impurity of quantum resource. To experimentally reconstruct the covariance matrix, the amplitude and phase quadratures of considered optical modes are measured, respectively, to obtain the diagonal elements of the matrix, and the correlation variances between the amplitude and phase quadratures of different modes are measured to obtain the nondiagonal elements[54] (see "Methods" for details).

The steerability of Bob by Alice ($A\to B$) for a two-mode Gaussian state with Gaussian measurement can be quantified by[55]:

$$\mathcal{G}^{A\to B}(\sigma_{AB})=\max\left\{0,\frac{1}{2}\ln\frac{\det\mathbf{A}}{\det\sigma_{\mathrm{AB}}}\right\}. \tag{4}$$

The quantity $\mathcal{G}^{A\to B}$ vanishes if the state described by σ_{AB} is nonsteerable by Gaussian measurements. The steerability of Alice by Bob ($B\to A$), quantified by $\mathcal{G}^{B\to A}$, can be obtained by replacing the role of A by B.

It is worth mentioning that the first criterion for the demonstration of the EPR paradox was proposed by M. Reid[56], and it was linked to the concept of steering lately[57]. For a two-mode Gaussian state, the quantifier as given by Eq. (4) is equivalent to the Reid's criterion which is based on Heisenberg uncertainty relation, i.e., a state is steerable from Alice to Bob if the following relation is violated:

$$V_{X_B|X_A}V_{P_B|P_A}\geq 1, \tag{5}$$

where $V_{X_B|X_A}$ and $V_{P_B|P_A}$ are the conditional variances of Bob's measurements conditioned on Alice's results, and $V_{X_B|X_A}V_{P_B|P_A}=\det\sigma_{AB}/\det\mathbf{A}$. For steering from Bob to Alice, the roles of A and B are swapped. This criterion does not require the assumption of Gaussian states or Gaussian systems to be valid.

At first, we investigate the effect of purity of quantum state on EPR steering. The purity of a quantum state ϱ is $\mu(\varrho)=\mathbf{Tr}\varrho^2$[18], which varies in the range of $\frac{1}{D}\leq\mu\leq 1$, where $D=\dim\mathcal{H}$ for a given Hilbert space $\mathcal{H}$. The minimum is reached by the totally random mixture, the upper bound is saturated by pure states. In the limit of CV systems ($D\to\infty$), the minimum purity tends to 0. The purity of any N-mode Gaussian state is only function of the symplectic eigenvalues υ_i of covariance matrix σ[58], which is given by:

$$\mu(\varrho)=\frac{1}{\prod_i\upsilon_i}=\frac{1}{\sqrt{\det\sigma}}. \tag{6}$$

Regardless of the number of modes, the purity of a Gaussian state is fully determined by the global symplectic invariant $\det\sigma$ alone[58].

In practice, the loss and noise in the generation system will lead to generation of impure quantum states[47,59]. For example, the phonon noise in the three-color entangled state prepared by a nondegenerate optical parametric oscillator (OPO) is a type of classical and uncorrelated noise, which leads to an impure three-color entangled state. Scattered light by thermal phonons inside a second-order nonlinear crystal is the source of additional phase noise observed in OPOs[47,59]. For our TMSS, the relationship between purity $\mu(\varrho)$ and δ is:

$$\mu(\varrho)=\frac{1}{\sqrt{\det\sigma_{AB}}}=\frac{1}{V_sV_{as}}=\frac{e^{2r}}{e^{2r}+\delta}. \tag{7}$$

The scheme of the transmission of Gaussian EPR steering in a lossy channel for pure and impure TMSSs is shown in Fig. 1a. Mode $\hat{B}$ of the TMSS is distributed in a lossy channel, the mode after transmission is given by $\hat{B}_L=\sqrt{\eta_L}\hat{B}+\sqrt{1-\eta_L}\hat{v}$, where η_L and $\hat{v}$ represent the transmission efficiency of quantum channel and the vacuum mode induced by loss into the quantum channel, respectively.

Second, the transmission of Gaussian EPR steering in a noisy channel is investigated, as shown in Fig. 1b, where the excess noise higher than the vacuum noise exists. Mode $\hat{B}$ of the TMSS is distributed in the noisy channel, the mode after transmission is given by $\hat{B}_N=\sqrt{\eta_N}\hat{B}+\sqrt{(1-\eta_N)g}\hat{N}+\sqrt{1-\eta_N}\hat{v}$, where $\hat{N}$ and g are the Gaussian noise in the channel with transmission efficiency of η_N and the magnitude of noise, respectively.

Finally, we demonstrate the revival of Gaussian EPR steering by establishing a correlated noisy channel, where an auxiliary channel carrying on the noise correlated with that of the noisy channel is

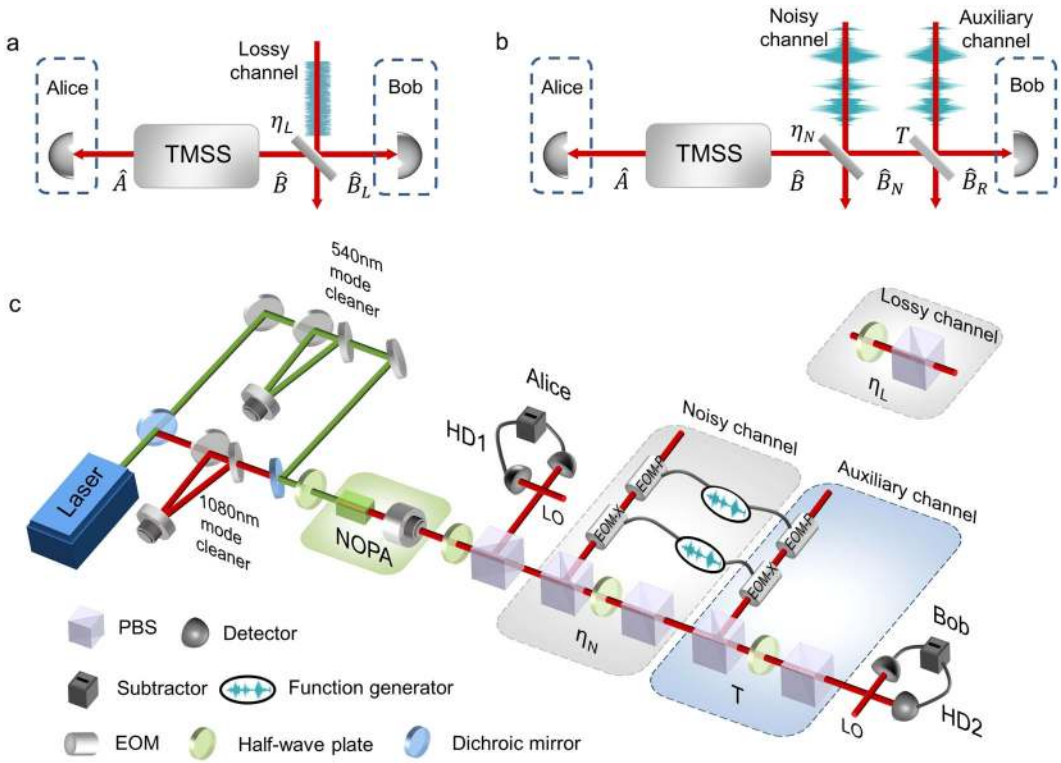

Fig. 1 The principle of experiment. a Schematic of EPR steering in lossy channel. One mode of the two-mode squeezed state (TMSS) $\hat{A}$ is kept by Alice, the other mode of TMSS $\hat{B}$ is distributed to Bob over a lossy channel which is experimentally mimicked by a beam splitter, the vacuum mode couples into system from the other input port of the beam splitter. The transmission efficiency of the lossy channel is η_L. **b** Schematic of disappearance and revival of EPR steering. Mode $\hat{B}$ is distributed to Bob over a noisy channel with an excess noise higher than the vacuum noise. The transmission efficiency of the noisy channel is η_N. An ancillary beam with noise correlated to noisy channel couples with the transmitted mode on a beam splitter with transmission coefficient T. **c** The experimental setup. A pure −3 dB TMSS at the sideband frequency of 3 MHz is generated by a nondegenerate optical parametric amplifier (NOPA). Alice and Bob perform homodyne measurement on their states, respectively. An ancillary beam is used to revive the EPR steering. PBS polarization beam splitter, LO local oscillator, EOM electro-optic modulator, HD homodyne.

introduced. In today's communication system, it is relevant to consider channels with correlated noise (i.e., non-Markovian environment), because the time- and space-correlated noise exists naturally[60–62]. Furthermore, it has been experimentally found that correlated noisy channel can be established by two bounded fibers[63], thus the method we use in experiment to build the non-Markovian environment is applicable and practical significant. As shown in Fig. 1b, the auxiliary noisy channel based on an ancillary coherent state $\hat{c}_{an}$, which is modulated to carry the noise information correlated with that in the noisy quantum channel, saying $\hat{c}'_{an} = \hat{c}_{an} + \sqrt{g_{an}}\hat{N}$ (g_{an} is the magnitude of the correlated noise and is experimentally adjustable). Thus there exists correlation between the quantum system and environment. The noisy transmitted mode $\hat{B}_N$ couples with the auxiliary noisy channel on a revival beam splitter with transmission efficiency T. One of the output mode we need from the revival beam splitter is $\hat{B}_R = \sqrt{\eta_N T}\hat{B} + \sqrt{(1-\eta_N)gT}\hat{N} - \sqrt{(1-T)g_{an}}\hat{N} + \sqrt{(1-\eta_N)T}\hat{v} - \sqrt{1-T}\hat{c}_{an}$, when the adjustable g_{an} and T satisfy:

$$\frac{g}{g_{an}} = \frac{1-T}{(1-\eta_N)T}, \tag{8}$$

it can be described as:

$$\hat{B}_R = \sqrt{\eta_N T}\hat{B} + \sqrt{(1-\eta_N)T}\hat{v} - \sqrt{1-T}\hat{c}_{an}. \tag{9}$$

Thus the excess noise in mode $\hat{B}_R$ can be removed totally, and the steerability between $\hat{B}_R$ and $\hat{A}$ can be revived to some degree.

Experimental setup

The experimental setup is shown in Fig. 1c. The loss in the quantum channel is experimentally mimicked by a beam splitter, which is composed by a half-wave plate and a polarization beam splitters (PBS), the vacuum mode couples into system from the other input port of the beam splitter. In the noisy environment, to couple the transmitted mode $\hat{B}$ and the noise-modulated coherent beam (auxiliary noisy channel $\hat{c}'_{an}$), the beam splitter (revival beam splitter) is composed by a PBS, a half-wave plate and another PBS as shown in Fig. 1c, where the transmission efficiency η_N and T are adjusted by setting the half-wave plate. The correlated noises between the quantum system and environment are generated by same signal generator experimentally. We reconstruct the covariance matrix of the quantum state with the homodyne detection systems, and quantify its steering properties.

The effect of purity on EPR steering

Figure 2 shows the effect of purity of the TMSS on EPR steering in a lossy channel, where the steerabilities quantified by two criteria given by Eqs. (4) and (5) are shown in Fig. 2a and 2b, respectively. For a pure −3 dB TMSS, one-way steering appears in a lossy channel, and the critical point of one-way steering property occurs at $\eta_L = 0.5$. For comparison, four different purities of the TMSSs at 0.8, 0.6, 0.4, and 0.2 are considered, which show that the maximum steerability and the phenomenon of one-way EPR steering property happens earlier with the decreasing of purity. This confirms that the impurity of the TMSS leads to decrease of steerabilities and two-way steering region. However, the

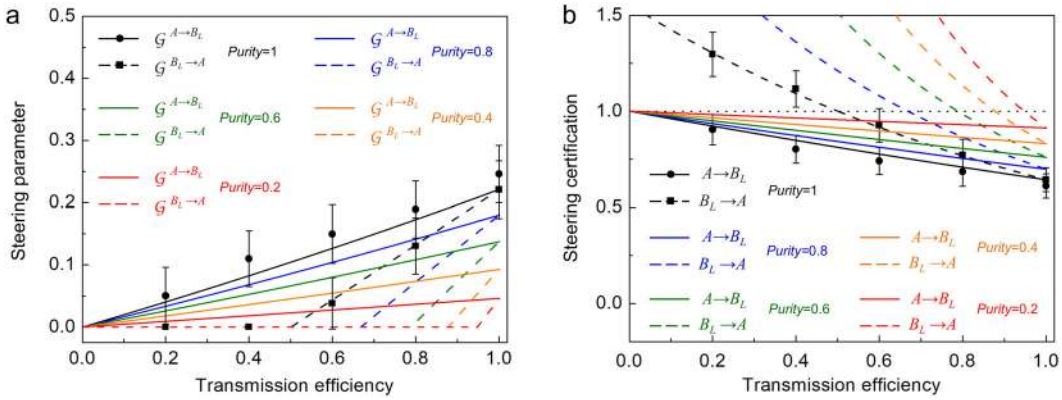

Fig. 2 The influence of purity of TMSS on the Gaussian EPR steering in a lossy channel. a Steering parameter quantified by Eq. (4). **b** Steering certification according to Eq. (5). The region under the bound of 1 (black dotted line) indicates the existence of steerability. Theoretical results for different purities of 1, 0.8, 0.6, 0.4, and 0.2 are considered, which correspond to different δ of 0, 0.5, 1.33, 2.99, and 7.97, respectively. The experimental data (black circles and squares) for the pure TMSS agree well with the theoretical prediction (black solid and dash curves). Error bars of experimental data represent ±1 standard deviation.

steerability from Alice to Bob never disappears until the purity tends to 0, which means that the impurity of the TMSS does not lead to sudden death of Gaussian EPR steering. The results in Fig. 2a and 2b confirm that two criteria given by Eqs. (4) and (5) are equivalent for a TMSS with Gaussian measurement in a lossy channel.

In the experiment, to determine the error bar of the experimental results, we measure three covariance matrices for each quantum state and obtain the corresponding EPR steering parameters. By calculating the mean value and the standard deviation of these three EPR steering parameters, error bars are obtained. The errors of the experimental data mainly come from the phase fluctuation of the phase locking system, and we take much effort to suppress phase fluctuation of each phase locking system to be $\theta \approx 1.5°$ by adjusting locking parameters.

The effect of noise on EPR steering

As shown in Fig. 3a and 3b, sudden death of Gaussian EPR steering of the TMSS in a noisy channel is observed, where the variance of the excess noise is taken as five times of vacuum noise. Specifically, in region I ($0.96 < \eta_N \le 1$), the two-way steering exists, both Alice and Bob can steer with each other. With the decreasing of η_N, when $0.86 < \eta_N \le 0.96$ (labeled as region II), one-way steering appears, i.e., Bob can steer Alice's state while Alice cannot steer Bob's state. More seriously, when $\eta_N \le 0.86$, the steerability between Alice and Bob totally disappeared (labeled as region III), i.e., the sudden death of the Gaussian EPR steering happens.

We also demonstrate sudden death of Gaussian EPR steering with different excess noise levels (noise levels are taken as 5, 10, 15, 20 times of vacuum noise) at fixed transmission efficiency ($\eta_N = 0.6$) in Fig. 3c, d. We can see the two-way steering (labeled as region I) and/or one-way steering (labeled as region II) could still exist when the excess noise is relatively low. When the variance of the excess noise is higher than 0.47 (labeled as region III), the sudden death of the Gaussian EPR steering happens. The results in Fig. 3 confirm that two criteria given by Eqs. (4) and (5) are equivalent for the sudden death and revival of Gaussian EPR steering of a TMSS with Gaussian measurement.

The effect of purity of initial TMSS on EPR steering in a noisy environment is also investigated as shown in Fig. 4. Figure 4a and 4b are the three-dimensional theoretical results of Gaussian EPR steering properties of initial TMSS with different purities of 1 and 0.8, respectively. It is obvious that the direction of EPR steering is changed with different noise levels, which is the same with the result in ref. [12]. We can see that the blue surface ($\mathcal{G}^{B_N \to A}$) and light red surface ($\mathcal{G}^{A \to B_N}$) have crossover, which happens with excess noise of 0.24 and 0.49 for the pure and impure TMSSs, respectively. Figure 4c shows the effect of purity of the TMSS on EPR steering in a noisy channel with excess noise of two times of vacuum noise. It is obvious that the sudden death of EPR steering for the impure state happens earlier and the maximum steerability is smaller than that of the pure state.

The revival of EPR steering

To revive the disappeared EPR steering, we fix $T = 0.9$ for the revival beam splitter and adjust the magnitude of correlated noise g_{an}. The parameters g/g_{an} are set to 0.14, 0.18, 0.28, and 0.56 for different quantum channel efficiencies of 0.2, 0.4, 0.6, and 0.8, respectively, according to Eq. (8). After the revival operation, the disappeared Gaussian EPR steering is revived as shown in Fig. 3a and 3b. Because the excess noise in mode $\hat{B}_R$ is removed totally in the revival operation, the Gaussian EPR steering is revived even at the noise level of 20 times of vacuum noise, as shown in Fig. 3c and 3d. Generally, T is better to be close to 1, because it results in adding an extra linear loss on the revived mode, this is why the steerabilities between mode $\hat{B}_R$ and $\hat{A}$ are not good as that between mode $\hat{B}_L$ and $\hat{A}$ (the pure lossy transmitted regime, presented by blue dash and solid curves in Fig. 3a).

DISCUSSION

Note that the noise in quantum channel and the noise in initial TMSS have different influences on EPR steerability. With the decreasing of purity of initial TMSS, the maximum steerability decreases and the phenomenon of one-way EPR steering property happens earlier than that of the pure state (between $0.5 \le \eta \le 1$), but the death of the EPR steering never happens. While with the increasing of noise in the quantum channel, the two-way EPR steering first declines to one-way EPR steering, and the sudden death of the Gaussian EPR steering finally occurs. Thus we can distinguish where the excess noise exists (whether in the communication channel or in the initial TMSS) by the Gaussian EPR steerability easily.

The sudden death of Gaussian EPR steering is different from that of the Gaussian entanglement, which is characterized by the positive partial transposition (PPT) criterion[64] (see "Methods" for details). Figure 5 shows the entanglement and steering region parameterized by transmission efficiency and excess noise, where the purple region represents the two-way steering region, the cyan region represents the one-way steering region of $\mathcal{G}^{A \to B}$, the light red region represents the one-way steering region of $\mathcal{G}^{B \to A}$,

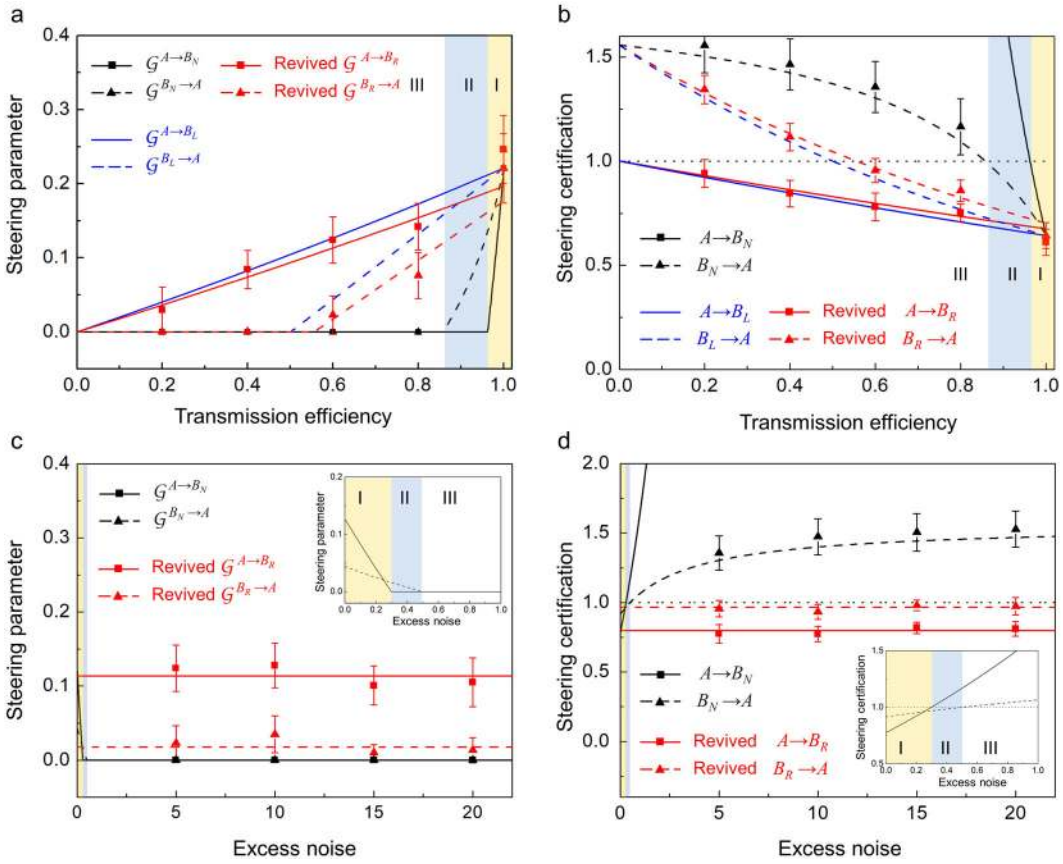

Fig. 3 Disappearance and revival of EPR steering in noisy channel. a, b Steering parameters quantified by Eqs. (4) and (5) in a noisy channel where the variance of the excess noise is taken as five times of vacuum noise, respectively. Black dash and solid curves are the theoretical predictions of $\mathcal{G}^{B_N\to A}$ and $\mathcal{G}^{A\to B_N}$, respectively. Region I, two-way steering; region II, one-way steering; region III, no steering. Red dash and solid curves are the theoretical predictions of $\mathcal{G}^{B_R\to A}$ and $\mathcal{G}^{A\to B_R}$ after steering revival, respectively. The blue dash and solid curves are the theoretical predictions of $\mathcal{G}^{B_L\to A}$ and $\mathcal{G}^{A\to B_L}$ in a pure lossy but noiseless channel. **c, d** Steering parameters quantified by Eqs. (4) and (5) in a transmission efficiency fixed ($\eta_N = 0.6$) noisy channel with different noise levels. Black dash and solid curves are theoretical predictions of $\mathcal{G}^{B_N\to A}$ and $\mathcal{G}^{A\to B_N}$ as a function of the excess noise in the unit of shot noise level. Red dash and solid curves are the theoretical predictions of $\mathcal{G}^{B_R\to A}$ and $\mathcal{G}^{A\to B_R}$ after steering revival, respectively. The inset figure shows the detailed theoretical predictions of $\mathcal{G}^{B_R\to A}$ and $\mathcal{G}^{A\to B_R}$ when the excess noise is relatively low. Error bars of experimental data represent ±1 standard deviation and are obtained based on the statistics of the measured data.

and the yellow region represents the entanglement without steering region, respectively. First, the direction of the EPR steering is changed with the increase of excess noise which is not the case in entanglement sudden death. The sudden death of EPR steering and entanglement happens when there is excess noise in the quantum channel. For a pure −3 dB TMSS, the direction of EPR steering is changed when the excess noise is 0.25 times of vacuum noise. This result comes from the intrinsic asymmetric character of EPR steering. Second, it is obvious that the sudden death of Gaussian EPR steering happens earlier than that of the entanglement with same excess noise level. Third, different from entanglement, the sudden death of Gaussian EPR steering in a noisy channel is directional.

Recovering EPR steering with correlated noisy channel can only remove the effect of excess noise in the transmission channel, the effect of loss in the transmission channel cannot be removed. Some other technologies such as noiseless linear amplification can be used to eliminate the effect of loss[65–68]. Recently, it has been shown that the measurement-based noiseless linear amplification can be used to distill Gaussian EPR steering in both lossy and noisy channels, which provides another feasible way to recover Gaussian EPR steering in quantum channel[69].

Comparing the present work of EPR steering revival with a correlated noisy channel and distillation of EPR steering with measurement-based NLA, the differences are as following. First, the steering revival with a correlated noisy channel can only remove the effect of excess noise in the quantum channel, the effect of loss in the transmitted channel cannot be removed. But the distillation of EPR steering works for both lossy and noisy channels. Second, the revival of Gaussian EPR steering with a correlated noisy channel can remove the excess noise in the quantum channel totally, but distillation of EPR steering with measurement-based NLA cannot remove the excess noise in all range of transmission efficiency (orange curves in Fig. 6). Third, the revived steerability with a correlated noisy channel cannot exceed the initial steerability (that in a pure lossy channel), but the distilled steerability can exceed the initial steerability.

Combining the methods of correlated noisy channel and the NLA may provide an option to distill Gaussian EPR steering in lossy and noisy environment. As shown in Fig. 6, if the measurement-based NLA based on Bob's measurement results with gain of 1.2 is applied after the revival of Gaussian EPR steering with a correlated noisy channel, the revived steerability could be enhanced by using the measurement-based NLA. In this case, the revival of steering with a correlated noisy channel removes the effect of excess noise in quantum channel. Followed by the measurement-based NLA, the effect of loss in quantum channel can be eliminated and the distillation of Gaussian steering can be obtained.

Our work demonstrates the evolution of bipartite Gaussian EPR steering of a TMSS transmitted in lossy and noisy quantum

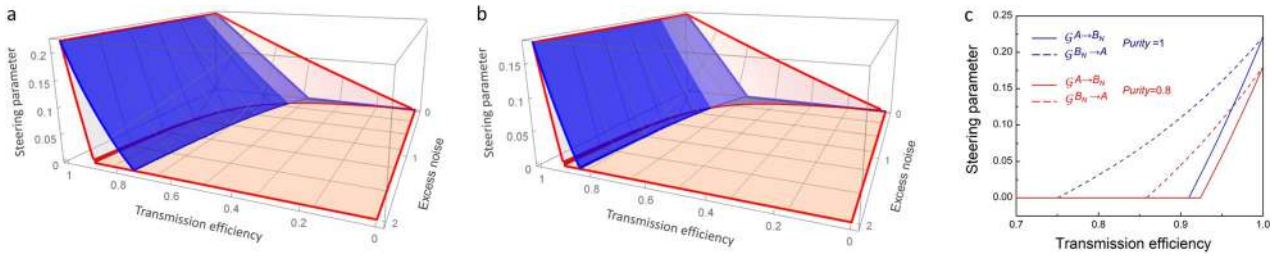

Fig. 4 Results for the effect of purity of the TMSS on EPR steering in a noisy channel. a, **b** The dependence of Gaussian EPR steering on transmission efficiency and excess noise with initial pure and impure (purity is 0.8) TMSS, respectively. The steerabilities of $\mathcal{G}^{A\to B_N}$ and $\mathcal{G}^{B_N\to A}$ are given by the light red and blue colors, respectively. **c** The effect of noise on EPR steering of the TMSS with purities of 1 (blue curves) and 0.8 (red curves), respectively. The excess noise is taken as two times of vacuum noise.

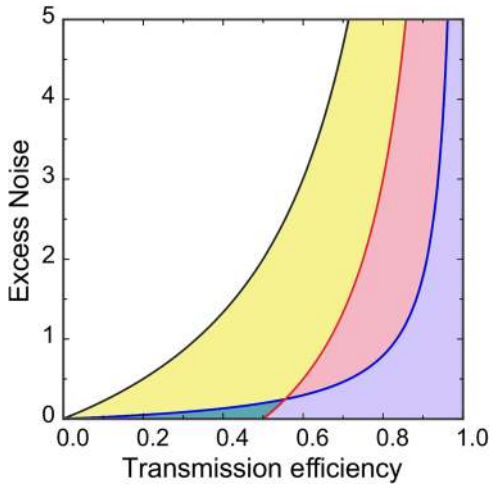

Fig. 5 The region plot parameterized by transmission efficiency and excess noise. The region below the black curve, which is the bound of entanglement sudden death, represents the existence of the entanglement. The region below the blue and red curves, which are the bound of the disappearance of $\mathcal{G}^{A\to B}$ and $\mathcal{G}^{B\to A}$, respectively, represents the existence of EPR steering.

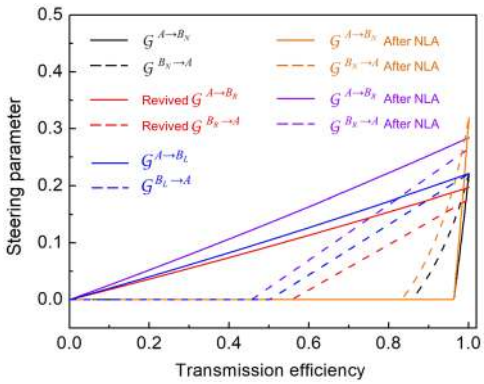

Fig. 6 Results for distillation of Gaussian steering with a correlated noisy channel and measurement-based NLA. Black solid and dash curves are the theoretical predicted steerabilities in a noisy channel with excess noise five times of vacuum noise. Red solid and dash curves are the predicted steerabilities after revival of Gaussian steering with a correlated noisy channel. The orange and purple curves are the predicted steerabilities when the measurement-based NLA based on Bob's measurement results with gain of 1.2 is applied before and after the revival of Gaussian steering, respectively. The blue solid and dash curves are the predicted steerabilities in a pure lossy but noiseless channel.

communication channels. We show the noise in quantum channel and the noise in the initial state result in different influences on EPR steerability. The impurity of the state only decreases the steerabilities and two-way steering region, but never leads to sudden death of EPR steering. While the excess noise in the quantum channel leads to sudden death of Gaussian EPR steering. We successfully revive EPR steering after the sudden death occurs in noisy channel by establishing a correlated noisy channel. The presented results provide useful references for understanding the steering properties of quantum state which interacts with different environments, also have potential applications in asymmetric quantum information processing exploiting EPR steering as a valuable resource.

METHODS

Covariance matrix of the TMSS

Gaussian state is the state with Gaussian characteristic functions and quasi-probability distributions in quantum phase space, which can be completely characterized by a covariance matrix. The elements of the bipartite covariance matrix are $\sigma_{ij} = Cov(\hat{R}_i, \hat{R}_j) = \frac{1}{2}\langle \hat{R}_i\hat{R}_j + \hat{R}_j\hat{R}_i\rangle - \langle \hat{R}_i\rangle\langle \hat{R}_j\rangle$, $i, j = 1$–4, where $\hat{R} = (\hat{x}_A, \hat{p}_A, \hat{x}_B, \hat{p}_B)^T$ is a vector composed by the amplitude and phase quadratures of bipartite optical beams[18]. Thus the TMSS covariance matrix can be partially expressed as (the cross-correlations between different quadratures of one mode are taken as 0):

$$\sigma = \begin{bmatrix} \triangle^2\hat{x}_A & 0 & \mathrm{Cov}(\hat{x}_A, \hat{x}_B) & 0 \\ 0 & \triangle^2\hat{p}_A & 0 & \mathrm{Cov}(\hat{p}_A, \hat{p}_B) \\ \mathrm{Cov}(\hat{x}_A, \hat{x}_B) & 0 & \triangle^2\hat{x}_B & 0 \\ 0 & \mathrm{Cov}(\hat{p}_A, \hat{p}_B) & 0 & \triangle^2\hat{p}_B \end{bmatrix}. \tag{10}$$

To partially reconstruct all relevant entries of its associated covariance matrix, we perform six different measurements on the output optical modes. These measurements include the amplitude and phase quadratures of the output optical modes $\triangle^2\hat{x}_A, \triangle^2\hat{p}_A, \triangle^2\hat{x}_B, \triangle^2\hat{p}_B$, and the cross-correlations $\Delta^2(\hat{x}_A + \hat{x}_B)$ and $\Delta^2(\hat{p}_A - \hat{p}_B)$. The covariance elements are calculated via the identities[54]:

$$\begin{aligned} \mathrm{Cov}(\hat{R}_i, \hat{R}_j) &= \tfrac{1}{2}\left[\Delta^2(\hat{R}_i + \hat{R}_j) - \Delta^2\hat{R}_i - \Delta^2\hat{R}_j\right], \\ \mathrm{Cov}(\hat{R}_i, \hat{R}_j) &= -\tfrac{1}{2}\left[\Delta^2(\hat{R}_i - \hat{R}_j) - \Delta^2\hat{R}_i - \Delta^2\hat{R}_j\right]. \end{aligned} \tag{11}$$

As an example, the partially reconstructed covariance matrix of the experimentally prepared pure TMSS is:

$$\sigma_{AB} = (1.260 - 0.79001.2800.80 - 0.7901.32000.8001.28). \tag{12}$$

For the TMSS distributed over lossy channel in the experiment we have:

$$\begin{aligned} \alpha_L &= \tfrac{V_s + V_{as}}{2} \\ \beta_L &= \tfrac{\eta_L(V_s + V_{as})}{2} + 1 - \eta_L \\ \gamma_L &= \tfrac{\sqrt{\eta_L}(V_s - V_{as})}{2} \end{aligned} \tag{13}$$

Furthermore, the TMSS distributed over noisy channel is:

$$\begin{aligned} a_N &= \tfrac{V_s+V_{as}}{2} \\ \beta_N &= \tfrac{\eta_N(V_s+V_{as})}{2} + (1-\eta_N)(g+1) \\ \gamma_N &= \tfrac{\sqrt{\eta_N}(V_s-V_{as})}{2} \end{aligned} \tag{14}$$

After the revival operation, the covariance matrix of the revived state is:

$$\begin{aligned} a_R &= \tfrac{V_s+V_{as}}{2} \\ \beta_R &= \tfrac{\eta_N T(V_s+V_{as})}{2} + 1 - \eta_N T \\ \gamma_R &= \tfrac{\sqrt{\eta_N T}(V_s-V_{as})}{2} \end{aligned} \tag{15}$$

With these theoretical and experimentally partially reconstructed covariance matrixes, we can quantify the Gaussian EPR steering of quantum states.

The PPT criterion[64] is applied to characterize the entanglement, which is a sufficient and necessary condition for a Gaussian TMSS. The PPT value can be determined by:

$$\sqrt{\frac{\Gamma - \sqrt{\Gamma^2 - 4\det\sigma_{AB}}}{2}}, \tag{16}$$

where $\Gamma = \det\mathbf{A} + \det\mathbf{B} - 2\det\mathbf{C}$. When the PPT value is <1, the two modes are entangled.

Details of experiment

Our experimental setup is shown in Fig. 1c, we use a nondegenerate optical parametric amplifier (NOPA) to prepare the TMSS. NOPA is pumped by a continuous-wave intracavity frequency-doubled Nd:YAP-LBO laser with two output wavelengths at 540 and 1080 nm. The NOPA consists of an *a*-cut type-II KTP crystal which is front face coated (work as the input coupler with transmittance of 21.2% and 0.04% at 540 and 1080 nm, respectively) and a concave mirror (work as the output coupler with transmittance of 0.5% and 12.5% at 540 and 1080 nm, respectively). Via the frequency down-conversion process of the pump field at 540 nm inside the NOPA which operated at deamplification condition (the relative phase between the pump laser and the injected signal equals to $(2n+1)\pi$), the TMSS at 1080 nm we want can be generated. Experimentally, the TMSS we prepared is a nearly pure −3.0 dB state at sideband frequency of 3 MHz.

DATA AVAILABILITY

The data that support the findings of this study are available from the corresponding author upon reasonable request.

Received: 1 October 2020; Accepted: 19 March 2021;
Published online: 27 April 2021

REFERENCES

1. Bell, J. S. On the Einstein-Podolsky-Rosen paradox. *Physics* **1**, 195–200 (1964).
2. Schrödinger, E. Discussion of probability relations between separated systems. *Math. Proc. Camb. Philos. Soc.* **31**, 555–563 (1935).
3. Schrödinger, E. Probability relations between separated systems. *Math. Proc. Camb. Philos. Soc.* **32**, 446–452 (1936).
4. Cavalcanti, D. & Skrzypczyk, P. Quantum steering: a review with focus on semidefinite programming. *Rep. Prog. Phys.* **80**, 024001 (2017).
5. Uola, R., Costa, A. C. S., Nguyen, H. C. & Gühne, D. Quantum steering. *Rev. Mod. Phys.* **92**, 015001 (2020).
6. Reid, M. D. et al. Colloquium: the Einstein-Podolsky-Rosen paradox: from concepts to applications. *Rev. Mod. Phys.* **81**, 1727 (2009).
7. Horodecki, R., Horodecki, P., Horodecki, M. & Horodecki, K. Quantum entanglement. *Rev. Mod. Phys.* **81**, 865 (2009).
8. Wiseman, H. M., Jones, S. J. & Doherty, A. C. Steering, entanglement, nonlocality, and the Einstein-Podolsky-Rosen paradox. *Phys. Rev. Lett.* **98**, 140402 (2007).
9. Händchen, V. et al. Observation of one-way Einstein-Podolsky-Rosen steering. *Nat. Photonics* **6**, 596–599 (2012).
10. Armstrong, S. et al. Multipartite Einstein-Podolsky-Rosen steering and genuine tripartite entanglement with optical networks. *Nat. Phys.* **11**, 167–172 (2015).
11. Deng, X. et al. Demonstration of monogamy relations for Einstein-Podolsky-Rosen steering in Gaussian clusterstates. *Phys. Rev. Lett.* **118**, 230501 (2017).
12. Qin, Z. et al. Manipulating the direction of Einstein-Podolsky-Rosen steering. *Phys. Rev. A* **95**, 052114 (2017).
13. Cai, Y., Xiang, Y., Liu, Y., He, Q. & Treps, N. Versatile multipartite Einstein-Podolsky-Rosen steering via a quantum frequency comb. *Phys. Rev. Res.* **2**, 032046(R) (2020).
14. Cavalcanti, D. et al. Detection of entanglement in asymmetric quantum networks and multipartite quantum steering. *Nat. Commun.* **6**, 7941 (2015).
15. Wollmann, S., Walk, N., Bennet, A. J., Wiseman, H. M. & Pryde, G. J. Observation of genuine one-way Einstein-Podolsky-Rosen steering. *Phys. Rev. Lett.* **116**, 160403 (2016).
16. Sun, K. et al. Experimental quantification of asymmetric Einstein-Podolsky-Rosen steering. *Phys. Rev. Lett.* **116**, 160404 (2016).
17. Xiao, Y. et al. Demonstration of multisetting one-way Einstein-Podolsky-Rosen steering in two-qubit systems. *Phys. Rev. Lett.* **118**, 140404 (2017).
18. Adesso, G. & Illuminati, F. Entanglement in continuous-variable systems: recent advances and current perspectives. *J. Phys. A Math. Theor.* **40**, 7821 (2007).
19. Weedbrook, C. et al. Gaussian quantum information. *Rev. Mod. Phys.* **84**, 621 (2012).
20. Bartkiewicz, K., Černoch, A., Lemr, K., Miranowicz, A. & Nori, F. Experimental temporal quantum steering. *Sci. Rep.* **6**, 38076 (2016).
21. Bartkiewicz, K., Černoch, A., Lemr, K., Miranowicz, A. & Nori, F. Temporal steering and security of quantum key distribution with mutually unbiased bases against individual attacks. *Phys. Rev. A* **93**, 062345 (2016).
22. Chen, S. et al. Spatio-temporal steering for testing nonclassical correlations in quantum networks. *Sci. Rep.* **7**, 3728 (2017).
23. Cavaillès, A. et al. Demonstration of Einstein-Podolsky-Rosen steering using hybrid continuous- and discrete-variable entanglement of light. *Phys. Rev. Lett.* **121**, 170403 (2018).
24. Walschaers, M. & Treps, N. Remote generation of Wigner-negativity through Einstein-Podolsky-Rosen steering. *Phys. Rev. Lett.* **124**, 150501 (2020).
25. Branciard, C., Cavalcanti, E. G., Walborn, S. P., Scarani, V. & Wiseman, H. M. One-sided device-independent quantum key distribution: security, feasibility, and the connection with steering. *Phys. Rev. A* **85**, 010301 (2012).
26. Gehring, T. et al. Implementation of continuous-variable quantum key distribution with composable and one-sided-device-independent security against coherent attacks. *Nat. Commun.* **6**, 8795 (2015).
27. Walk, N. et al. Experimental demonstration of Gaussian protocols for one-sided device-independent quantum key distribution. *Optica* **3**, 634–642 (2016).
28. Kogias, I., Xiang, Y., He, Q. & Adesso, G. Unconditional security of entanglement-based continuous-variable quantum secret sharing. *Phys. Rev. A* **95**, 012315 (2017).
29. Xiang, Y., Kogias, I., Adesso, G. & He, Q. Multipartite Gaussian steering: monogamy constraints and quantum cryptography applications. *Phys. Rev. A* **95**, 010101(R) (2017).
30. Reid, M. D. Signifying quantum benchmarks for qubit teleportation and secure quantum communication using Einstein-Podolsky-Rosen steering inequalities. *Phys. Rev. A* **88**, 062338 (2013).
31. He, Q., Rosales-Zárate, L., Adesso, G. & Reid, M. D. Secure continuous variable teleportation and Einstein-Podolsky-Rosen steering. *Phys. Rev. Lett.* **115**, 180502 (2015).
32. Chiu, C.-Y., Lambert, N., Liao, T.-L., Nori, F. & Li, C.-M. No-cloning of quantum steering. *npj Quantum Inf.* **2**, 16020 (2016).
33. Huang, C.-Y., Lambert, N., Li, C.-M., Lu, Y.-T. & Nori, F. Securing quantum networking tasks with multipartite Einstein-Podolsky-Rosen steering. *Phys. Rev. A* **99**, 012302 (2019).
34. Piani, M. & Watrous, J. Necessary and sufficient quantum information characterization of Einstein-Podolsky-Rosen steering. *Phys. Rev. Lett.* **114**, 060404 (2015).
35. Chen, S.-L., Budroni, C., Liang, Y.-C. & Chen, Y.-N. Natural framework for device-independent quantification of quantum steerability, measurement incompatibility, and self-testing. *Phys. Rev. Lett.* **116**, 240401 (2016).
36. He, Q. Y. & Reid, M. D. Genuine multipartite Einstein-Podolsky-Rosen steering. *Phys. Rev. Lett.* **111**, 250403 (2013).
37. Cavalcanti, E. G., He, Q. Y., Reid, M. D. & Wiseman, H. M. Unified criteria for multipartite quantum nonlocality. *Phys. Rev. A* **84**, 032115 (2011).
38. Li, C.-M. et al. Genuine high-order Einstein-Podolsky-Rosen steering. *Phys. Rev. Lett.* **115**, 010402 (2015).
39. Deng, X., Tian, C., Wang, M., Qin, Z. & Su, X. Quantification of quantum steering in a Gaussian Greenberger-Horne-Zeilinger state. *Opt. Commun.* **421**, 14–18 (2018).
40. Xiang, Y., Su, X., Mišta, Jr., L., Adesso, G. & He, Q. Multipartite Einstein-Podolsky-Rosen steering sharing with separable states. *Phys. Rev. A* **99**, 010104 (2019).
41. Wang, M. et al. Deterministic distribution of multipartite entanglement and steering in a quantum network by separable states. *Phys. Rev. Lett.* **125**, 260506 (2020).
42. Yu, T. & Eberly, J. H. Sudden death of entanglement. *Science* **323**, 598–601 (2009).
43. Almeida, M. P. et al. Environment-induced sudden death of entanglement. *Science* **316**, 579–582 (2007).

44. Barbosa, F. A. S. et al. Robustness of bipartite Gaussian entangled beams propagating in lossy channels. *Nat. Photonics* **4**, 858–861 (2010).
45. Barbosa, F. A. S. et al. Disentanglement in bipartite continuous-variable systems. *Phys. Rev. A* **84**, 052330 (2011).
46. Bartkowiak, M. et al. Sudden vanishing and reappearance of nonclassical effects: general occurrence of finite-time decays and periodic vanishings of nonclassicality and entanglement witnesses. *Phys. Rev. A* **83**, 053814 (2011).
47. Coelho, A. S. et al. Three-color entanglement. *Science* **326**, 823–826 (2009).
48. Deng, X., Tian, C., Su, X. & Xie, C. Avoiding disentanglement of multipartite entangled optical beams with a correlated noisy channel. *Sci. Rep.* **7**, 44475 (2017).
49. Xu, J. et al. Experimental demonstration of photonic entanglement collapse and revival. *Phys. Rev. Lett.* **104**, 100502 (2010).
50. Deng, X. et al. Disappearance and revival of squeezing in quantum communication with squeezed state over a noisy channel. *Appl. Phys. Lett.* **108**, 081105 (2016).
51. Kim, Y.-S., Lee, J. C., Kwon, O. & Kim, Y.-H. Protecting entanglement from decoherence using weak measurement and quantum measurement reversal. *Nat. Phys.* **8**, 117–120 (2012).
52. Yamamoto, N., Nurdin, H. I., James, M. R. & Petersen, I. R. Avoiding entanglement sudden death via measurement feedback control in a quantum network. *Phys. Rev. A* **78**, 042339 (2008).
53. Rosales-Zárate, L. et al. Decoherence of Einstein-Podolsky-Rosen steering. *J. Opt. Soc. Am. B* **32**, A82 (2015).
54. Steinlechner, S., Bauchrowitz, J., Eberle, T. & Schnabel, R. Strong Einstein-Podolsky-Rosen steering with unconditional entangled states. *Phys. Rev. A* **87**, 022104 (2013).
55. Kogias, I., Lee, A. R., Ragy, S. & Adesso, G. Quantification of Gaussian quantum steering. *Phys. Rev. Lett.* **114**, 060403 (2015).
56. Reid, M. D. Demonstration of the Einstein-Podolsky-Rosen paradox using nondegenerate parametric amplification. *Phys. Rev. Lett.* **40**, 913 (1989).
57. Cavalcanti, E. G., Jones, S. J., Wiseman, H. M. & Reid, M. D. Experimental criteria for steering and the Einstein-Podolsky-Rosen paradox. *Phys. Rev. A* **80**, 032112 (2009).
58. Adesso, G., Serafini, A. & Illuminati, F. Extremal entanglement and mixedness in continuous variable systems. *Phys. Rev. A* **70**, 022318 (2004).
59. César, J. E. S. et al. Extra phase noise from thermal fluctuations in nonlinear optical crystals. *Phys. Rev. A* **79**, 063816 (2009).
60. Kretschmann, D. & Werner, R. F. Quantum channels with memory. *Phys. Rev. A* **72**, 062323 (2005).
61. Corney, J. F. et al. Many-body quantum dynamics of polarization squeezing in optical fibers. *Phys. Rev. Lett.* **97**, 023606 (2006).
62. Lassen, M., Berni, A., Madsen, L. S., Filip, R. & Andersen, U. L. Gaussian error correction of quantum states in a correlated noisy channel. *Phys. Rev. Lett.* **111**, 180502 (2013).
63. Xu, J. et al. Robust bidirectional links for photonic quantum networks. *Sci. Adv.* **2**, e1500672 (2016).
64. Simon, R. Peres-Horodecki separability criterion for continuous variable systems. *Phys. Rev. Lett.* **84**, 2726 (2000).
65. Ralph, T. C. Quantum error correction of continuous-variable states against Gaussian noise. *Phys. Rev. A* **84**, 022339 (2011).
66. Xiang, G. Y., Ralph, T. C., Lund, A. P., Walk, N. & Pryde, G. J. Heralded noiseless linear amplification and distillation of entanglement. *Nat. Photonics* **4**, 316–319 (2010).
67. Chrzanowski, H. M. et al. Measurement-based noiseless linear amplification for quantum communication. *Nat. Photonics* **8**, 333–338 (2014).
68. Ulanov, A. E. et al. Undoing the effect of loss on quantum entanglement. *Nat. Photonics* **9**, 764–768 (2015).
69. Liu, Y. et al. Distillation of Gaussian Einstein-Podolsky-Rosen steering with noiseless linear amplification. *arXiv* 2004.14073v1. https://arxiv.org/abs/2004.14073 (2020).

ACKNOWLEDGEMENTS

This research was supported by the NSFC (Grant Nos. 11904160, 11834010, and 62005149), the program of Youth Sanjin Scholar, National Key R&D Program of China (Grant No. 2016YFA0301402), and the Fund for Shanxi "1331 Project" Key Subjects Construction.

AUTHOR CONTRIBUTIONS

X.S. and X.D. conceived the original idea and designed the experiment; X.D., Y.L., and M.W. carried out the experiment and analyzed the data; X.S., X.D., Y.L., and K.P. prepared the paper.

COMPETING INTERESTS

The authors declare no competing interests.

ADDITIONAL INFORMATION

Correspondence and requests for materials should be addressed to X.S.

Reprints and permission information is available at http://www.nature.com/reprints

Publisher's note Springer Nature remains neutral with regard to jurisdictional claims in published maps and institutional affiliations.

Open Access This article is licensed under a Creative Commons Attribution 4.0 International License, which permits use, sharing, adaptation, distribution and reproduction in any medium or format, as long as you give appropriate credit to the original author(s) and the source, provide a link to the Creative Commons license, and indicate if changes were made. The images or other third party material in this article are included in the article's Creative Commons license, unless indicated otherwise in a credit line to the material. If material is not included in the article's Creative Commons license and your intended use is not permitted by statutory regulation or exceeds the permitted use, you will need to obtain permission directly from the copyright holder. To view a copy of this license, visit http://creativecommons.org/licenses/by/4.0/.

© The Author(s) 2021